Project 2 for ME 820

Dept. Mech. & Nuclear Engineering

Bolun Xu

blxu@ksu.edu

May 10, 2019

In this project we are to simulate the incompressible flow in 2D squared cavity. I considered two different problems, one is lid-driven cavity flow, the other is thermal convection. Hereafter I briefly introduce the structure of this report. In section 1 the introduction of this code and the mesh design are presented, the results of lid-driven cavity flow is shown in section 2 and the thermal convection part will be discussed in section 3. All codes are in Fortran.

1 Instructions of the code & mesh information

First of all I would like to introduce the N-S solver, mainly about its structure as well as functions. The structure of this program is briefly shown in figure 1.

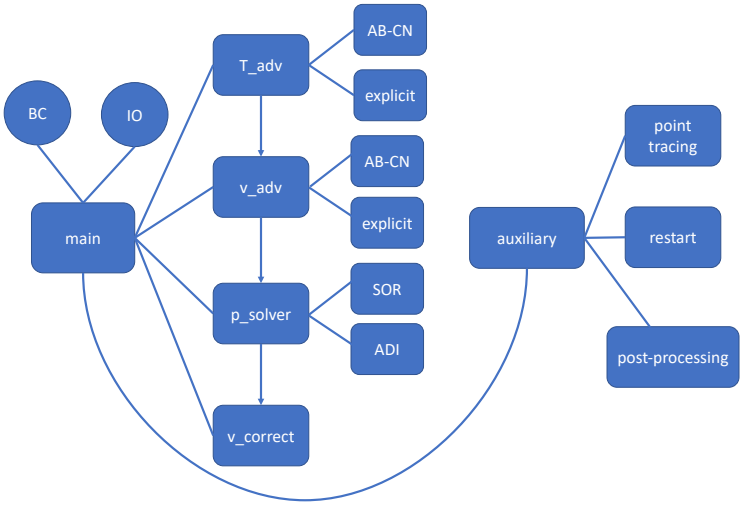

Figure 1: The structure of the program.

The whole procedure can be divided into 4 steps. Assuming we already have the flow field in nth step, firstly we solve the energy equation to obtain temperature T at $(n+1)$th step it thermal convection problem is dealt with. Then we temporally integrate momentum equation without pressure gradient term to get the intermediate velocity u^*. Next, solve pressure Poisson equation to get intermediate pressure. At last, using the gradient of the intermediate pressure to correct u^*, which projects it back to divergence-free field to get the velocity at $(n+1)$ step. For temporal advancing, several schemes

can be chosen including 1st-order Euler, 2nd-order Adams-Bashforth (AB2) and AB2 plus Crank-Nicholson (CN), which is a semi-implicit scheme. Note that all results present later were calculated by AB2-CN scheme, though the results of another two explicit methods were almost the same as the AB2-CN one. For pressure solver, SOR or ADI method can be used. Besides main N-S solver, some auxiliary subroutines may also useful, including point tracing function which can monitor the time series of flow variables at some fixed points in domain, and restart function which can continue the computation from previous time step, as well as some post-processing functions which can compute some physical quantities we are interested in.

The equations are discretized on a staggered mesh, the brief sketch of which is shown in figure 2. Basically all scalar variables including pressure and temperature are defined on the center of grid cell, while vector variables are defined on the center of grid line. For output, all the variables are interpolated onto grid point beforehand then only one mesh is needed for visualization, which is more convenient.

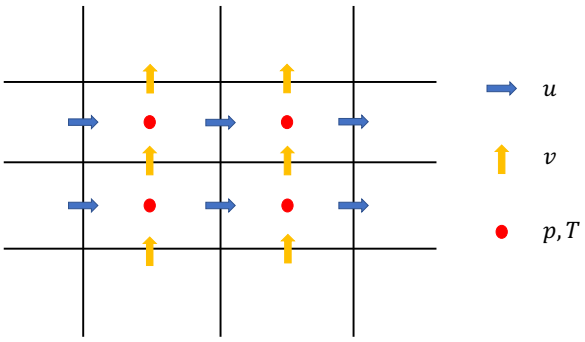

Figure 2: The staggered mesh

2 Lid-driven cavity flow

Firstly I will ntroduce the methodology applied in the solver, then present some results.

2.1 Methodology

I basically solve N-S equation by so-called fractional-step method, following the instruction in the paper [Kim & Moin(1985)]. The governing equations are

$$\begin{aligned} &\nabla \cdot \mathbf{u} = 0 \\ &\partial_t \mathbf{u} + \nabla \cdot (\mathbf{uu}) = -\nabla p + \frac{1}{Re}\nabla^2 \mathbf{u}. \end{aligned} \tag{1}$$

Although 1st-order and 2nd-order fully explicit schemes were also used in my code, I would rather introduce 2-step time-advancement method only here. The scheme for equation 1 is

$$\frac{u_i^* - u_i^n}{\Delta t} = \frac{1}{2}(3H_i^n - H_i^{n-1}) + \frac{1}{2Re}(L_x + L_y)(u_i^* + u_i^n) \tag{2}$$

$$u_i^{n+1} - u_i^* = -\Delta t \partial_i p^{n+1}. \tag{3}$$

In this scheme AB2 is used for advective term and CN is used for viscous term, where H_i means advective term, L_x and L_y are finite difference operators for 2nd-order derivative. Equation 2 can be rearranged as

$$(1 - \frac{\Delta t}{2Re}L_x - \frac{\Delta t}{2Re}L_y)(u_i^* - u_i^n) = \frac{\Delta t}{2}(3H_i^n - H_i^{n-1}) + 2(\frac{\Delta t}{2Re}L_x + \frac{\Delta t}{2Re}L_y)u_i^n \tag{4}$$

In this equation we can find the terms in right-hand side are all known, and the linear operator in left-hand side constructs a 5-point stencil. Such linear system is solvable but may be time-consuming. So we used approximate factorization technique to simplify the computation. [Warming & Beam(1979)]. The left-hand side of equation 4 can be approximated as

$$(1 - \frac{\Delta t}{2Re}L_x)(1 - \frac{\Delta t}{2Re}L_y)(u_i^* - u_i^n) = \frac{\Delta t}{2}(3H_i^n - H_i^{n-1}) + 2(\frac{\Delta t}{2Re}L_x + \frac{\Delta t}{2Re}L_y)u_i^n \tag{5}$$

After such treatment, we instead solve two tridiagonal systems, which can be solved quickly by Thomas algorithm. Next step is to determine the pressure at intermediate time step, note that this pressure p is not the true pressure with physical meaning, it can be merely regarded as an intermediate scalar. This p can be obtained by solving Poisson equation

$$(\frac{\partial^2}{\partial x^2} + \frac{\partial^2}{\partial y^2})p = \frac{1}{\Delta t}\partial_i u_i^*. \tag{6}$$

For this equation I used simple Neumann boundary condition, which is $\partial p / \partial n = 0$. In order to obtain the true pressure field, the following equation

is used [Brown *et al.*(2001)Brown, Cortez & Minion]:

$$P^{n+1} = p + \frac{\Delta t}{2Re}(\frac{\partial^2}{\partial x^2} + \frac{\partial^2}{\partial y^2})p \tag{7}$$

The final step is to project the intermediate velocity field back to divergence-free field, namely by

$$u_i^{n+1} = u_i^* - \Delta t \partial_i p \tag{8}$$

2.2 Results

First I validated my code by comparing my results with the benchmark given in previous literatures. Figure 3 shows the u profile along $x = 0.5L$ line when $Re = 400$. We can find my results match the results of Kim & Moin [Kim & Moin(1985)] pretty well, proving my code is reliable.

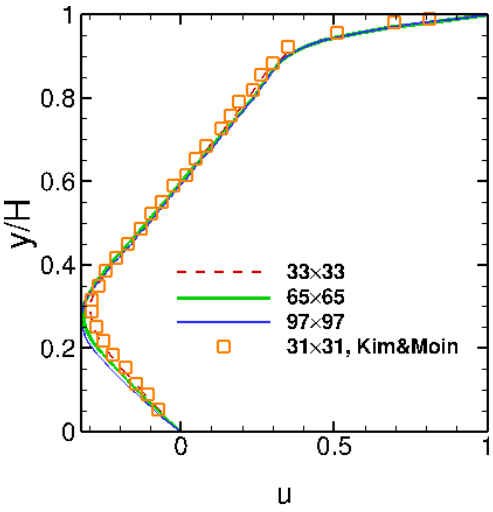

Figure 3: The u profile along centerline $x = 0.5L$

Figure 4 shows the velocity and pressure fields when Re is not very high. 65 by 65 mesh is used. When Re is moderate, the flow keeps steady. Basically a main roll is formed in the bulk of cavity. Also two small vortex can be observed near the bottom corners. The whole system is not symmetric that the right corner vortex is bigger than the left one.

When Re increases, some new phenomena happen in the cavity. Figure 5 shows the u profile along centerline $x = 0.5L$ for different sizes of mesh when $Re = 5000$. It can be found the results of 129×129, 257×257 and 385×385 are quite close, implying the results are already independent of mesh. So I

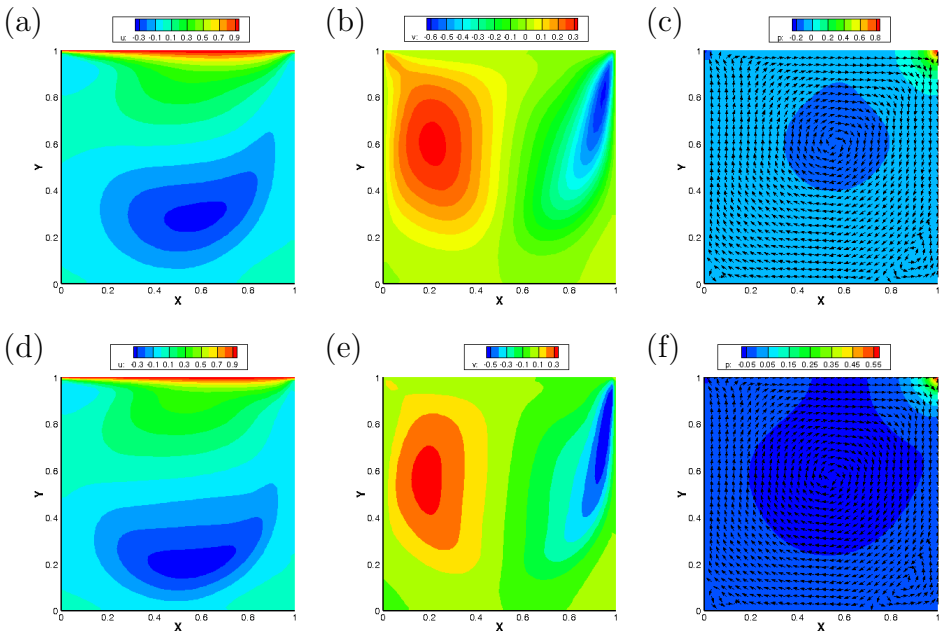

Figure 4: The contours for u, v and p with velocity vectors. (a)-(c): $Re = 400$; (d)-(f): $Re = 1000$.

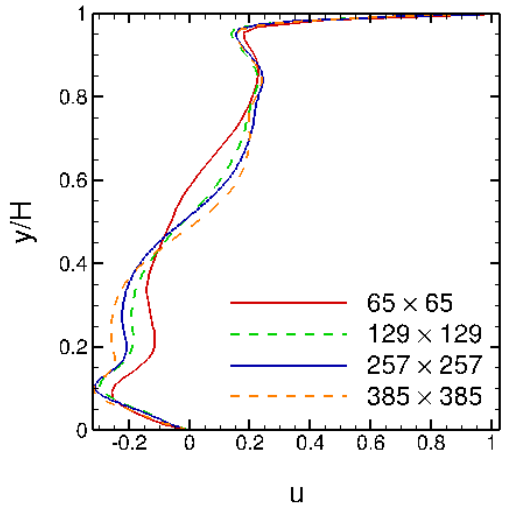

Figure 5: The u profile along centerline $x = 0.5L$ for different mesh sizes when $Re = 5000$.

chose 257×257 for the computation of higher Re. Figure 6 shows the velocity and pressure fields when $Re = 5000$ and $Re = 10000$. From figure 6 ((a) & (d)) it can be seen the boundary becomes thinner when Re increases, which is consistent with the physics. When Re is high more vortex appearing in the cavity, as we can observe in figure 6(f), a vortex is generated near the left wall, which is also observed by Ghia *et al.* [Ghia *et al.*(1982)Ghia, Ghia & Shin]. In addition, when $Re = 10000$ the flow is unsteady. Figure 7 shows the time-series of velocity at a monitoring point $(0.5L, 0.8H)$. We can find the velocity signals need longer time to converge to steady state.

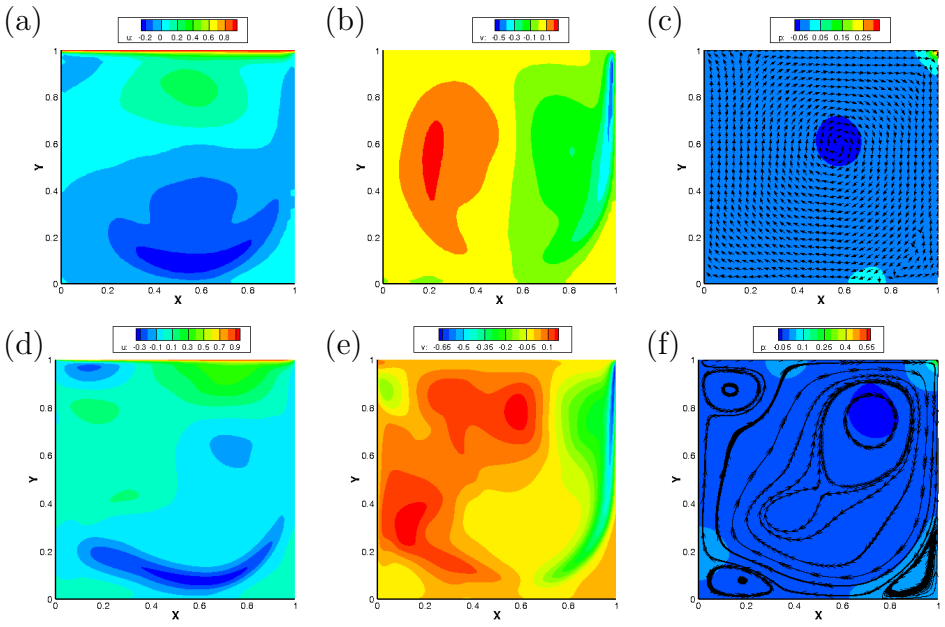

Figure 6: The contours for u, v and p with velocity vectors. (a)-(c): $Re = 5000$; (d)-(f): $Re = 10000$.

3 Thermal convection

3.1 Methodology & Background

For thermal convection problem, energy equation must be involved in solving procedure. Here we firstly consider a canonical thermal convection called Rayleigh-Bénard convection, which the flow is heated uniformly from bottom and cooled from top at the same time, whilst all the walls of the cavity are stationary. To describe this problem properly, the N-S equation together

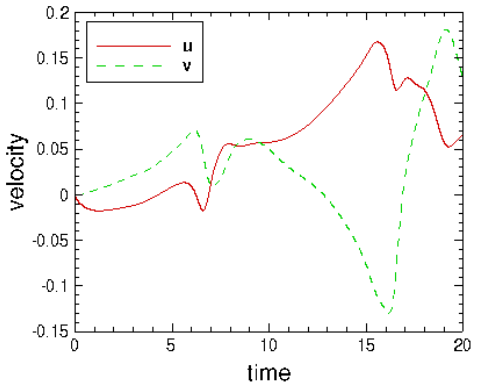

Figure 7: The time-series of velocity at monitoring point $(0.5L, 0.8H)$ when $Re = 10000$.

with energy equation can be written as follow

$$\nabla \cdot \mathbf{u} = 0 \tag{9}$$

$$\partial_t \mathbf{u} + \nabla \cdot (\mathbf{u}\mathbf{u}) = -\nabla p + \sqrt{\frac{Pr}{Ra}} \nabla^2 \mathbf{u} + T\mathbf{e}_y \tag{10}$$

$$\partial_t T + \nabla \cdot (\mathbf{u}T) = \frac{1}{\sqrt{RaPr}} \nabla^2 T, \tag{11}$$

where Ra is Rayleigh number which means the ratio of buoyancy force to viscous force, and Pr the Prandtl number which means the ratio of viscous diffusivity to thermal diffusivity. In my computation Pr is fixed to 0.71, which is the Pr of ideal gas at room temperature.

The time-advancement of momentum equation is almost the same as I did when solving driven cavity flow, the only difference is to discretize buoyancy term explicitly. For energy equation, AB2 is used for advective term and CN is used for heat conduction term. Also approximate factorization method is implemented for faster solving.

When Ra is quite small, which means the buoyancy force in the system is very weak, there is no convection in the cavity because of the strong viscous effect impeding the flow motion. Then the heat is transported only through conduction, when the equilibrium state is reached, the temperature distribution in the cavity is an linear function of height of the cavity, which can be obtained both theoretically and numerically, as shown in figure 8.

As Ra is increasing, once the buoyancy force is strong enough to overcome the stabilizing effect brought by viscous force, the convection happens. The Ra at that threshold is called critical Ra, which differs from system to system.

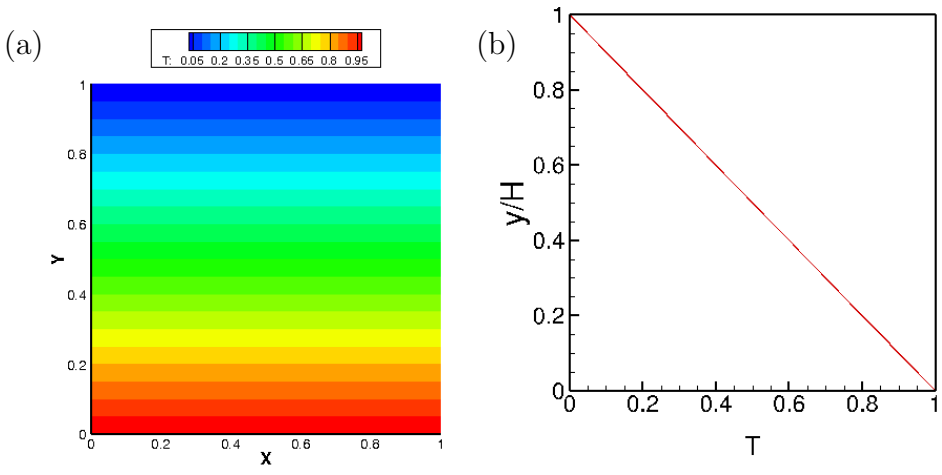

Figure 8: Conduction solution when Ra is below the critical value. (a): The contours of T; (b): T profile along y.

Although in my project the critical Ra is not precisely sought, based on other literatures and my experience this value should be in the range $(10^3, 10^4)$. So hereafter I use $Ra = 10^4, 10^5, 10^6$ for simulation.

There are two responding parameters in thermal convection system. One is Reynolds number which indicates the flow strength in the whole system, However I don't intend to discuss Re here. Another one is Nusselt number Nu which indicates the heat flux in the cavity. There are several ways to calculate Nu, all of which should give an identical result. Here I use

$$Nu = -\int_{bottom} \frac{\partial T}{\partial y} dx \tag{12}$$

to determine Nu.

3.2 Results

Figure 9 shows the results of simulation for $Ra = 10^4$. 65×65, 129×129 and 257×257 meshes were used in simulation while the results shown here are in 129×129 mesh. From figure 9(c) we can find my result matches the benchmark in [Ouertatani *et al.*(2008)Ouertatani, Cheikh, Beya & Lili] well. It can be observed the hot fluid goes up and the cold goes down to form a convection roll in the bulk. The whole system is perfectly symmetric, and the temperature in the bulk remains the average of top and bottom temperature. This is also an essential feature of Rayleigh-Bénard convection.

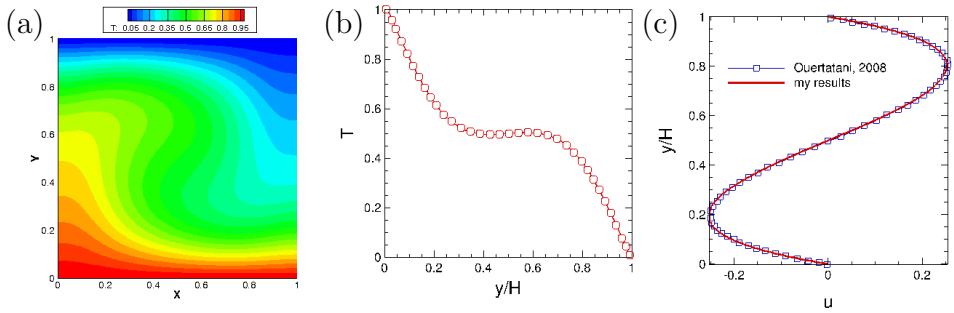

Figure 9: Results for $Ra = 10^4$. (a): The contours of T; (b): Horizontal averaged T profile along y; (c): u profile along centerline $x = 0.5L$. Blue line with symbols are results from [Ouertatani *et al.*(2008)Ouertatani, Cheikh, Beya & Lili]

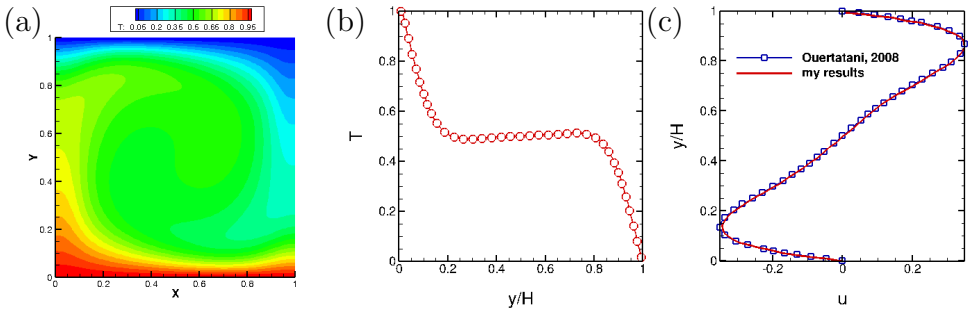

Figure 10: Results for $Ra = 10^5$. (a): The contours of T; (b): Horizontal averaged T profile along y; (c): u profile along centerline $x = 0.5L$. Blue line with symbols are results from [Ouertatani *et al.*(2008)Ouertatani, Cheikh, Beya & Lili]

Figure 10 shows the results for $Ra = 10^5$. Also without surprise, from figure 10(c) we can find my result matches the benchmark in [Ouertatani *et al.*(2008)Ouertatani, Cheikh, Beya & Lili] well. From figure 10(b) it can be found that the temperature changes more quickly near the top and bottom plate, which means the thermal boundary layer becomes thinner as Ra grows.

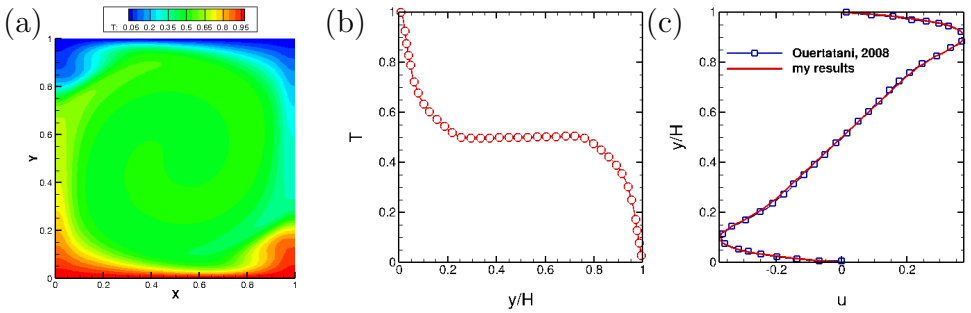

Figure 11: Results for $Ra = 10^6$. (a): The contours of T; (b): Horizontal averaged T profile along y; (c): u profile along centerline $x = 0.5L$. Blue line with symbols are results from [Ouertatani *et al.*(2008)Ouertatani, Cheikh, Beya & Lili]

Figure 10 shows the results for $Ra = 10^6$. Similar trends in velocity and temperature can still be observed at this Ra. As Ra becomes higher, it takes longer time for the flow field to reach the steady state. At much higher Ra, the flow will lose its stability for second time, usually it becomes unsteady, chaotic, and finally turbulent.

	present	literature
$Nu/Ra = 10^4$	2.196	2.158
$Nu/Ra = 10^5$	4.054	3.910
$Nu/Ra = 10^6$	6.681	6.309

Table 1: Nu for different Ra compared to the results in [Ouertatani *et al.*(2008)Ouertatani, Cheikh, Beya & Lili].

In table 1 I listed Nu for different Ra compared to the results in [Ouertatani *et al.*(2008)Ouertatani, Cheikh, Beya & Lili]. Unlike the velocity profile, I found the Nu doesn't match that well with the benchmark. One possible reason is the accuracy of my integral subroutine is too rough to calculate a precise Nu. I may try more ways to calculate Nu then compare the results of each.

4 Thermal convection with shearing on the top plate

In this section I consider shearing effect brought by moving top plate in RB convection. The lid speed fixed to 1. The results for $Ra = 10^4$ are present in figure 12. We find due to the shearing effect, the symmetry of the system is broken, the boundary layer near the top becomes much thicker than the one near the bottom. Nu is 3.147, which is higher than pure RB case. It indicates the shearing promotes the heat transfer in the system.

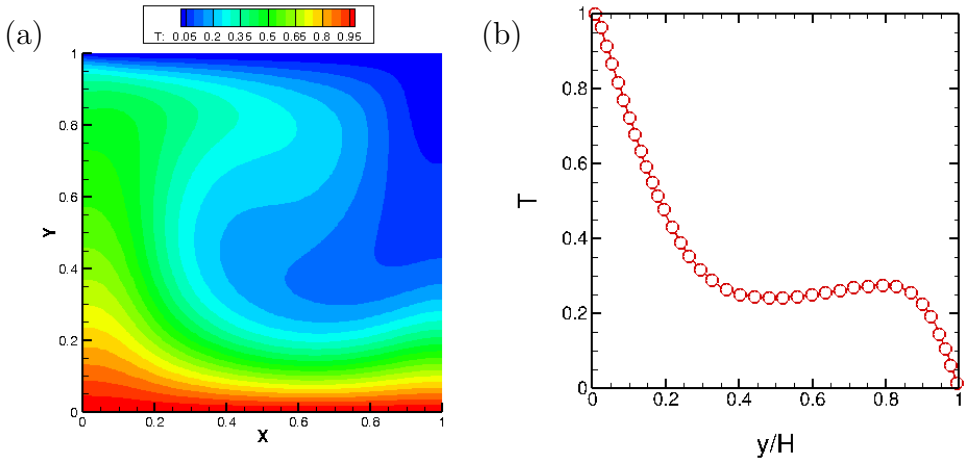

Figure 12: Results of RB convection with moving plate for $Ra = 10^4$. (a): The contours of T; (b): Horizontal averaged T profile along y.

5 Conclusion

In this project a numerical solver using finite difference method for incompressible NS equation and energy equation has been developed, with several numerical schemes available in code. The solver can compute lid-driven cavity and thermal convection problem. Some results are given, and in overall they can match the benchmarks in literatures.

References

[Brown *et al.*(2001)Brown, Cortez & Minion] Brown, David L, Cortez, Ricardo & Minion, Michael L 2001 Accurate projection methods

for the incompressible Navier–Stokes equations. *Journal of computational physics* **168** (2), 464–499.

[Ghia *et al.*(1982)Ghia, Ghia & Shin] Ghia, UKNG, Ghia, Kirti N & Shin, CT 1982 High-Re solutions for incompressible flow using the Navier-Stokes equations and a multigrid method. *Journal of computational physics* **48** (3), 387–411.

[Kim & Moin(1985)] Kim, John & Moin, Parviz 1985 Application of a fractional-step method to incompressible Navier-Stokes equations. *Journal of computational physics* **59** (2), 308–323.

[Ouertatani *et al.*(2008)Ouertatani, Cheikh, Beya & Lili] Ouertatani, Nasreddine, Cheikh, Nader Ben, Beya, Brahim Ben & Lili, Taieb 2008 Numerical simulation of two-dimensional Rayleigh–Bénard convection in an enclosure. *Comptes Rendus Mécanique* **336** (5), 464–470.

[Warming & Beam(1979)] Warming, RF & Beam, Richard M 1979 An extension of a-stability to alternating direction implicit methods. *BIT Numerical Mathematics* **19** (3), 395–417.